



Article

Scenario-Based Extreme Flood Risk of Residential Buildings and Household Properties in Shanghai

Xinmeng Shan ¹, Jiahong Wen ^{1,*}, Min Zhang ^{1,2}, Luyang Wang ¹, Qian Ke ³ , Weijiang Li ¹, Shiqiang Du ^{1,4} , Yong Shi ⁵, Kun Chen ¹, Banggu Liao ¹, Xiande Li ¹ and Hui Xu ¹

¹ School of Environmental and Geographical Sciences, Shanghai Normal University, Shanghai 200234, China; mxshan_123@163.com (X.S.); zhangmin@shnu.edu.cn (M.Z.); wmhd01@163.com (L.W.); Lwj@shnu.edu.cn (W.L.); shiqiangdu@shnu.edu.cn (S.D.); kun_1949301@126.com (K.C.); Liaomap@163.com (B.L.); Lixiande2007@163.com (X.L.); xuhui@shnu.edu.cn (H.X.)

² State Key Laboratory of Estuarine and Coastal Research, East China Normal University, Shanghai 200062, China

³ Department of Hydraulic Engineering, Delft University of Technology, 1 Stevinweg, 2628 CN Delft, The Netherlands; Q.ke@tudelft.nl

⁴ Institute of Urban Studies, Shanghai Normal University, Shanghai 200234, China

⁵ Department of Tourism and Management, University of Zhengzhou, Zhengzhou 450001, China; yongshi@zzu.edu.cn

* Correspondence: jhwen@shnu.edu.cn

Received: 7 May 2019; Accepted: 4 June 2019; Published: 8 June 2019



Abstract: Extreme flooding usually causes huge losses of residential buildings and household properties, which is critical to flood risk analysis and flood resilience building in Shanghai. We developed a scenario-based multidisciplinary approach to analyze the exposure, losses and risks of residential buildings and household properties, and their spatial patterns at the neighborhood committee level in Shanghai, based on extreme storm flood scenarios of 1/200, 1/500, 1/1000 and 1/5000-year. Our findings show that the inundation area of the residential buildings caused by a 1/200-year storm flood reaches 24.9 km², and the total loss of residential buildings and household properties is 29.7 billion CNY (Chinese Yuan) (or 4.4 billion USD), while the inundation area of residential buildings and the total loss increases up to 162.4 km² and 366.0 billion CNY (or 54.2 billion USD), respectively for a 1/5000-year storm flood. The estimated average annual loss (AAL) of residential buildings and household properties for Shanghai is 590 million CNY/year (or 87.4 million USD/year), with several hot spots distributed around the main urban area and on the bank of the Hangzhou Bay. Among sixteen districts, Pudong has the highest exposure and annual expected loss, while the inner city is also subject to extreme flooding with an AAL up to near half of the total. An analysis of flood risk in each of 209 subdistricts/towns finds that those most vulnerable to storm flooding are concentrated in Pudong, Jiading, Baoshan Districts and the inner city. Our work can provide meaningful information for risk-sensitive urban planning and resilience building in Shanghai. The methodology can also be used for risk analysis in other coastal cities facing the threat of storm flooding.

Keywords: extreme flooding; residential building; household property; risk analysis; Shanghai

1. Introduction

Floods affecting Shanghai are usually categorized into fluvial, pluvial and coastal storm flooding. However, the primary risk of flooding to the Shanghai city is from the sea. Located at the mouth of the Yangtze River, Shanghai is one of the most exposed coastal megacities to extreme flooding, caused by a typhoon induced storm surge in combination with a high astronomic tide, heavy rain, and a fluvial

flood [1–8]. Moreover, climate change, sea level rise, land subsidence and rapid urban growth will significantly increase the risk of extreme flooding for Shanghai in the future [1,2,4,5,9–12]. Therefore, understanding the risk and implementing effective risk-reduction measures to manage and mitigate the risk are urgently needed for urban sustainable development in Shanghai.

In recent years, flood risks in Shanghai have been highlighted in the field of flood risk analysis and management [7,11,13–15]. Many studies conducted the hazard simulation of fluvial and pluvial floods [8,10,16], and assessed the exposure, vulnerability, loss and risk to floods for a neighborhood committee (NC) or district scale in Shanghai municipality [14,17–20]. In particular, the extreme flood risk with low-probability and high consequence has been focused in recent decades because it can cause catastrophic damage and losses for the city's social, economic sectors, infrastructure and environment as well [1,4,11,21–25].

Residential buildings and household properties are key assets for people living in flood prone areas, and their damage and risks caused by flooding have been focused by many previous studies [26–31]. The total area of residential buildings in Shanghai is 672.8 km², with an average price of 54.2 thousand CNY per square meter [32], hence a total asset is up to 36,465.8 billion CNY. Meanwhile, the value of household properties has dramatically increased due to great improvement of the resident's living quality. The economic losses of residential buildings and household properties caused by flooding has also increased significantly [14,33], which becomes an essential component of flood risk analysis in Shanghai [20,34]. Several studies have been focused on the flood risk analysis for the residential buildings and household properties in recent years. A study by Wu et al. [34] mapped the building asset value and estimated the exposure and loss for the whole Shanghai, based on a single 1/1000-year storm flood scenario with no embankments provided by Ke [1]. Other studies were conducted for pluvial and fluvial flooding locally at the NC or subdistrict level [14,18–20,33].

However, a city-scale study of the risks of residential buildings and household properties caused by extreme flooding is still to be accomplished in Shanghai for two major reasons. First, city scale inundation maps caused by extreme flooding under different return periods were not available. Second, the asset distributions of residential buildings and household properties in Shanghai were not mapped. In recent years, we made great efforts to develop an integrated numerical simulation system, coupling the atmosphere (Fujita typhoon model), ocean model (TELEMAC tidal model and TOMAWAC wave model) and coastal model (MIKE11 river network model and MIKE21 two-dimensional hydrodynamic model) [35]. The simulation system was employed to generate four inundation maps caused by extreme flooding under 1/200, 1/500, 1/1000 and 1/5000-year scenarios, respectively. Meanwhile, thanks to the rapid development of the Internet, open source data [36], and wide application of artificial intelligence in disaster risk assessment [37–39], we mapped the housing price for Shanghai at the neighborhood committee (NC) level [40], and developed reliable space-explicit datasets of residential buildings and household properties in Shanghai, using machine learning [40] to combine a variety of online datasets. These advances made it feasible for us to analyze exposure, losses and risks for residential buildings and household properties caused by extreme flooding at the NC level in the whole city of Shanghai, and to identify their spatial patterns with a spatial statistic method [17,41] in this study.

2. Data and Methods

2.1. Study Area

Shanghai is the biggest metropolis and economic center in China, with an area of 6340 km² and a population up to 24.2 million in 2017. The whole city situates in a flat and low-lying coastal region with an average elevation of about 4 m. It's surrounded by waters on three sides, with the Huangpu River and the Suzhou Creek passing through the city (Figure 1a). The city is affected by typhoons almost every year with a frequency of 1.5 times per year [42].

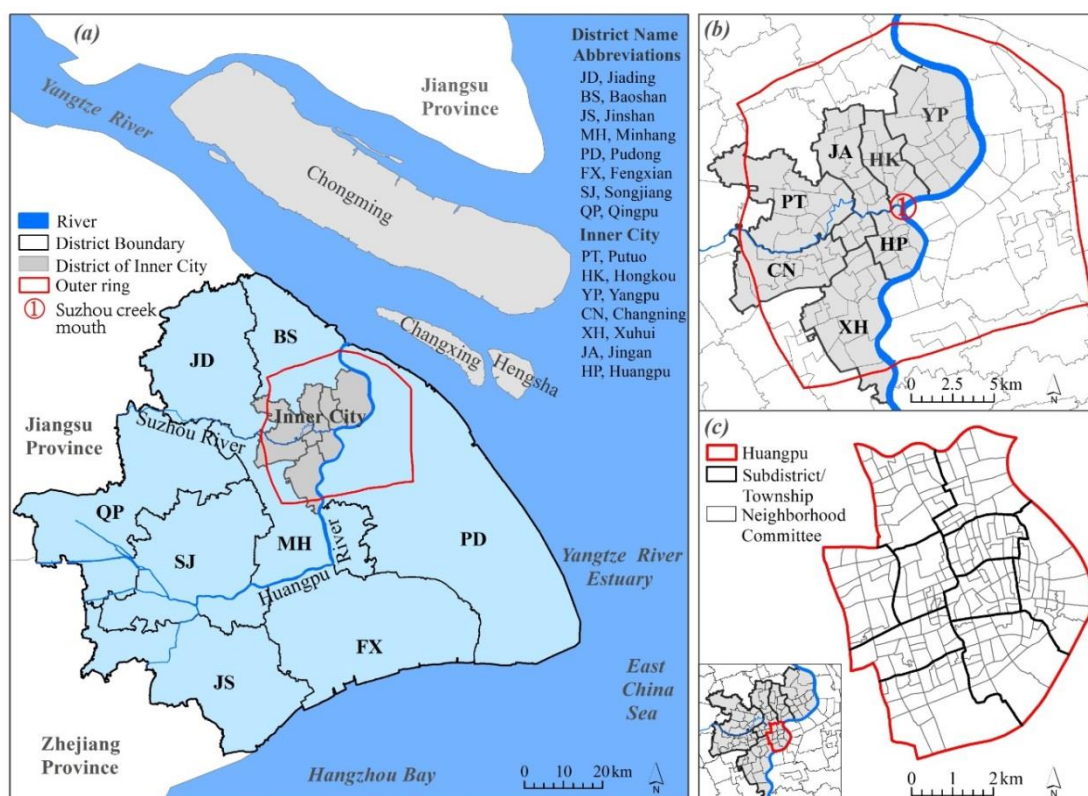


Figure 1. Study area (the light blue area of Shanghai city, with an exception of Chongming, Changxing and Hengsha Islands in light grey (a)), the inner city within the outer ring in red (b), and the hierarchy levels of district, subdistrict/township and neighborhood committee in Huangpu District (c).

This study takes Shanghai city as a study area, with the exception of Chongming District (including Chongming, Changxing and Hengsha islands) (Figure 1a). The study area consists of 15 districts, 209 subdistricts/towns and 5088 NCs. NCs are the smallest administrative unit in cities of China, which play a fundamental role in urban risk management [17,43]. Eight downtown districts are located on the west of the Huangpu River in the inner city area (within the outer ring) (Figure 1b). Taking Huangpu District as an example, the hierarchy levels of district, subdistrict/township and neighborhood committee are shown in Figure 1c.

2.2. Data

The data used in this work mainly include four extreme flood scenarios, Shanghai residential building data, housing price data and market price data of household properties in 2017.

Aerts et al. [21] selected low-probability extreme surge events with return periods of 40 years and longer to model flood risk for New York City for the current climate conditions. Shanghai has higher-standard flood protection measures [5], such as sea walls with a 200-year coastal flood return level design that protect its coastal area, and flood walls with 1000-year riverine flood return level along the Huangpu River to protect the city from riverine flooding [5]. However, the 1/1000-year protection level, approved by the Ministry of Water Resources and Shanghai Municipal People's Government in 1984, may decrease due to combined factors of subsidence, sea level and the hydrological change of the Huangpu River [44,45]. In order to identify flood hazard in extreme events, Ke [1] performed a frequency analysis of annual maximum water levels, using a generalized extreme value (GEV) distribution. The results turned out that the current estimation of overtopping probability is 1/200-year in the Huangpu River [1].

Therefore, we selected the return period of extreme flood scenarios equal to or longer than 200 years. First, an integrated numerical simulation system, coupling the atmosphere (Fujita typhoon

model), ocean model (TELEMAC and TOMAWAC) and coastal model (MIKE11 and MIKE21), was developed, calibrated and validated to simulate the extreme flooding [35,46,47]. The simulation system was then employed to provide four inundation scenarios of (Figure 2) the extreme water levels caused by storm tide as a function of 1/200, 1/500, 1/1000 and 1/5000-year, respectively combined with a fluvial flood during Typhoon TC9711 in 1997 [4,35]. A DTM (digital terrain model) with an original grid size of 10 m by 10 m was used for our coastal model [35]. The area covered by the buildings was not excluded from the calculation domain, which appears as blocks with the height of 20 m in the DTM. The spatial resolution of 60 m by 60 m was finally applied for the MIKE21 model due to limited computational resources. The frequency analysis of annual maximum water levels was performed, using the generalized extreme value (GEV) distribution to estimate the extreme water levels for different return periods [1,48]. The inundation period is in line with the time frame of Typhoon TC9711. The crest height of sea dikes and floodwalls along the Huangpu River were taken into account and the failure mechanisms of the flood defense system were overflowing and overtopping. The inundation depth of each residential building is derived by averaging the water depths from grids of the simulation outcomes neighboring the building footprints.

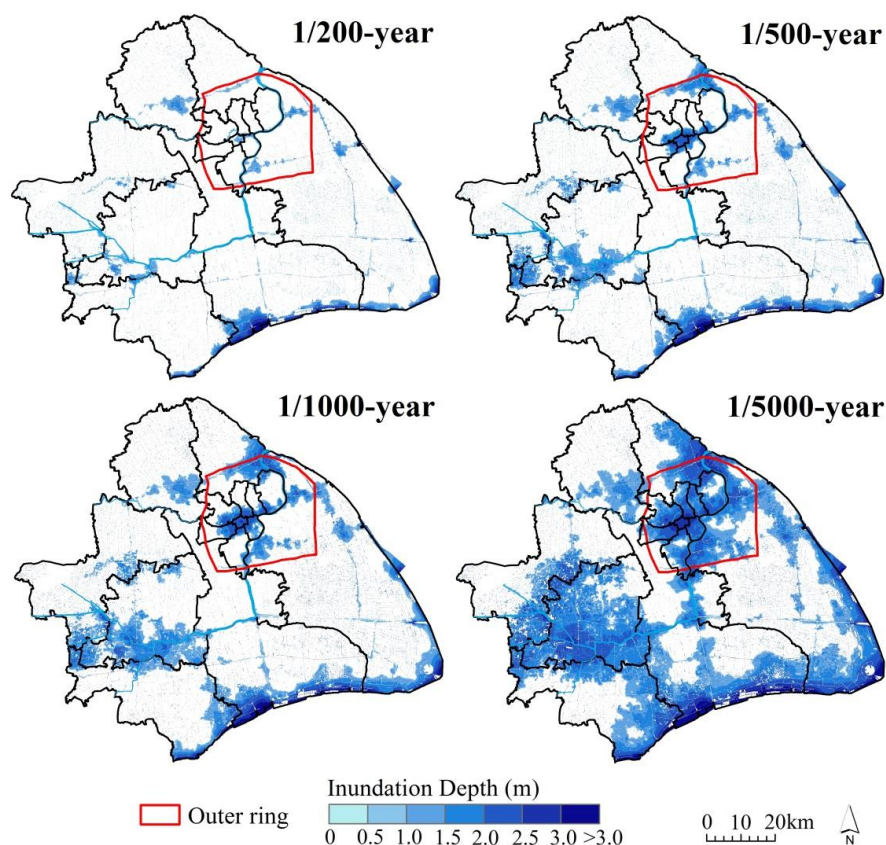


Figure 2. Inundation maps with extent and maximum depth caused by extreme flooding as a function of return periods in Shanghai city (excluding the area of islands).

The data of Shanghai residential buildings in 2017 include the building's footprint and height information, which were acquired from Baidu Map (<https://map.baidu.com>) using a python-based web crawler, and then processed by a GIS software. The accuracy of residential building footprint data was evaluated, using high-precision remote sensing images from Google Earth. A total of 150 NCs (10 NCs for each district) in the study area were randomly selected as validation samples. Residential buildings were interpreted visually from the Google Earth images, and compared with the footprint data from

Baidu Map. The results show that the overall accuracy of residential building footprint data in 2017 is 92.8% with a standard deviation of 3.2%, indicating that the footprint data have very high quality.

Another python-based web crawler was developed to retrieve the online information of the housing price in Shanghai in 2017, provided by Lianjia, a popular Chinese O2O (online-to-offline) real estate agency service provider (<https://sh.lianjia.com/>). Housing price data of 3562 NCs were then acquired after careful data processing to remove the invalid records or outliers. There were still 1526 NCs with no observed data. The boosting model XGBoost [49] was used to estimate housing prices for those areas [40] and a variable was created to represent the spatial correlation relationship to improve the model performance. A spatially explicit and consistent housing price dataset at the NC level for the study area is finally obtained [40].

The current market price data of household properties in 2017 were derived from price reports provided by the Shanghai Statistical Yearbook [32] and company websites of household appliances and furniture (<http://www.zol.com.cn/>), and Shanghai household decoration. The market price data of household appliances and furniture in 2017 are mainly derived from large O2O (online-to-offline) appliance sales companies, and furniture shopping malls in Shanghai.

2.3. Methods

A quantitative risk analysis process method is developed (Figure 3) based on four basic elements for assessing risk: Hazard, exposure, vulnerability and loss [50]. First, the assets of residential buildings and household properties are estimated and mapped at the NC level, based on the information of residential building area, housing price, floor number and household property values. Second, the assets exposed to floods are obtained by overlay analysis of the asset maps with the hazard maps of extreme storm floods. Third, the losses of residential buildings and household properties within a specific flood scenario are estimated, based on the exposure and stage-damage functions. Finally, the risk, expressed as the estimated average annual loss (AAL), is quantified as a function of the probabilities of flood events (or return periods) and their potential losses. Only the ground floor was considered for assessing the exposure, losses and risks of residential buildings and household properties since inundation areas with depth greater than 3.0 m (exceeding the first storey) are less than 0.05% of the total flooded region in all four scenarios. The total exposure, losses and AALs at municipality, district and township levels are aggregated from the NC level.

2.3.1. Asset Value Analysis of Household Properties

The household properties mainly include wall coating, wooden floor, household appliances and furniture according to the Shanghai Statistical Yearbook 2017 and previous studies [14,18]. The current market price method is used to assess the asset value of household properties [51].

① Estimation of wall coating cost

The total cost per square meter is the sum of wall coating cost and labor cost. Following previous studies [14,18], the wall coating cost was estimated on the basis of the market price. The labor cost of wall coating was estimated according to the reference price information from the Shanghai household decoration market.

An empirical method was used to estimate the wall coating area for interior walls, i.e., the wall coating area is about 2.5 times of the building footprint area [14]. Therefore, the wall coating costs W [CNY] can be calculated as follows:

$$W = \sum_{i=1}^n (2.5 \times S_{\text{building}} \times M_1) \quad (1)$$

where 2.5 is an empirical factor [-]; S_{building} , the footprint area of residential buildings [m^2]; M_1 , the total cost of wall coating cost and labor cost per square meter [CNY/m^2].

② Estimation of wooden floor cost

The total wooden floor cost per square meter is the sum of the floor price and the labor cost [14]. The wooden floor cost F [CNY] can then be calculated using Equation (2).

$$F = \sum_{i=1}^n (S_{building} \times M_2) \quad (2)$$

where $S_{building}$ is the wooden floor area of the residential buildings [m^2]; M_2 is the sum of the wooden floor price and labor cost per square meter [CNY/ m^2].

③ Estimation of household appliances and furniture cost

The averaged asset values of household appliances and furniture for household were acquired by a sample survey. The number of households can be estimated by the area of residential buildings divided by the average household area [32], the cost P [CNY] of household appliances and furniture is estimated as follows [33]:

$$P = \sum_{i=1}^n (E + F) \times N \quad (3)$$

where E and F are the market price of major household appliances and furniture [CNY], respectively per household; N is the number of households [-].

Finally, the total asset and its distribution of household properties were estimated by aggregating the costs of wall coating, wooden floor, household appliances and furniture in all the NCs of Shanghai.

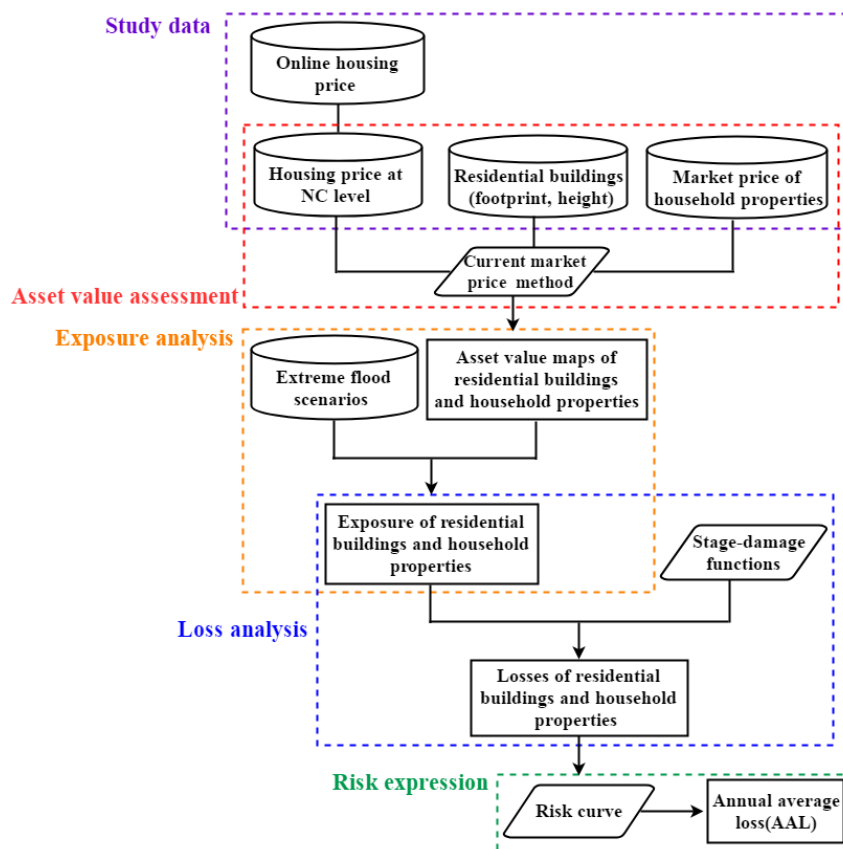


Figure 3. The methodology framework of flood risk analysis in this study.

2.3.2. Exposure Analysis

A GIS software was used to calculate the exposed assets by overlaying the hazard maps of extreme flooding with the asset distributions of residential buildings and household properties. The exposure of total asset E_{asset} [CNY] to storm flooding includes two parts: The exposed asset of residential buildings B [CNY] and the exposed asset of household properties C [CNY].

$$E_{\text{asset}} = B + C \quad (4)$$

where

$$C = W_1 + F_1 + P_1 \quad (5)$$

where W_1 , F_1 and P_1 are exposed assets of wall coating, wooden floor and household appliances and furniture [CNY], respectively, which were derived by overlay analysis to combine wall coating value W (Equation (1)), wooden floor value F (Equation (2)), and household appliances and furniture value P (Equation (3)) with four inundation scenarios caused by extreme flooding.

2.3.3. Loss Analysis

Losses of residential buildings and household properties under different storm flood scenarios were analyzed, respectively.

Loss Analysis of Residential Buildings

The stage-damage function developed by Ke [1] was used to evaluate the losses of residential buildings in this work (Figure 4a). The stage-damage function, derived by summarizing a variety of previous studies and empirical events in Shanghai [1], indicates the relationship of residential building loss rate with water depth at an interval of 0.5 m. The direct economic loss of residential buildings V [CNY] can be calculated as follows:

$$V = \sum_{i=1}^n (B \times R_1) \quad (6)$$

where B is the exposed asset of residential buildings [CNY]; R_1 is the loss rate of residential buildings under different inundation depths [-].

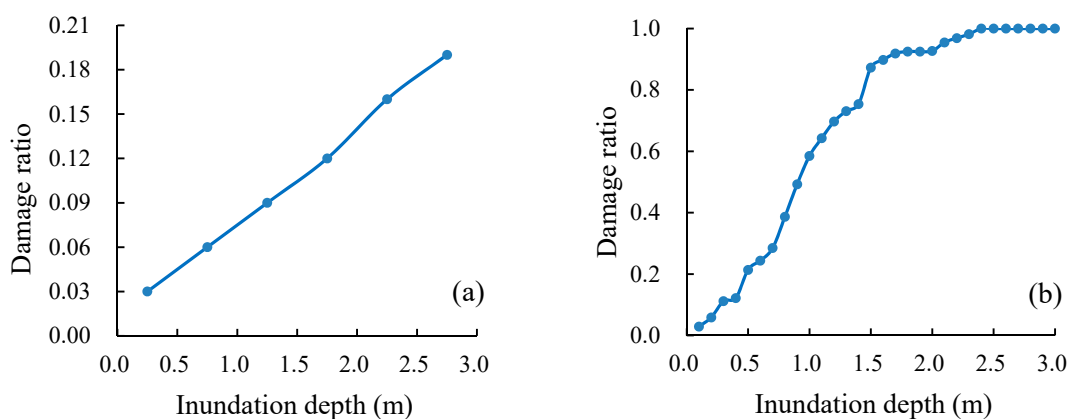


Figure 4. Stage-damage functions. (a) Residential buildings [1]; (b) household properties including wall coating, household appliances and furniture [33].

Loss Analysis of Household Properties

Previous studies show that the loss rates of household properties for different households tend to be similar, that is, the stage-damage functions are almost the same [14,18,33,52]. In this work, the stage-damage functions of wall coating (Figure 4b), wooden floor, household appliances and furniture

(Figure 4b) developed by Shi et al. [33] were used to estimate the loss values of household properties. These functions represented the relationship of household property loss rates with water depth at an interval of 0.1 m [33].

① Loss analysis of wall coating

The loss of wall coating, caused by water immersion, is composed of the repainting and labor costs. It's closely related to water depth, and can be formulated as follows:

$$Q = \sum_{i=1}^n (W_1 \times R_2) \quad (7)$$

where Q is the loss of wall coating [CNY]; W_1 is the exposed value of wall coating [CNY]; R_2 is the loss rate of wall coating under different water depths [-].

② Loss analysis of wooden floor

Wooden floor loss T [CNY] is distinct because it is usually assumed to have no direct relationship with water depth. Floor loss occurs once soaked. Therefore, T is equal to the exposed wooden floor asset F_1 [CNY].

$$T = F_1 \quad (8)$$

③ Loss analysis of household appliances and furniture

The loss of household appliances and furniture H [CNY] is closely related to water depth and can be calculated according to Equation (9).

$$H = P_1 \times R_2 \quad (9)$$

where P_1 is the total exposed assets of household appliances and furniture [CNY]; R_2 is the loss rate of household appliances and furniture under different water depths [-].

2.3.4. Risk Expression

Risk can be expressed as a curve, in which all scenarios are plotted with their return periods or probabilities and associated losses, and the curve can be used directly to calculate the expected average annual loss (AAL) [CNY/year].

$$AAL = \int x f(x) dx \quad (10)$$

where x is the losses [CNY]; $f(x)$ is the corresponding probabilities [-].

2.3.5. Spatial Pattern Identification

The local G_i^* statistic is used to quantify the spatial heterogeneity of the AAL, and it can be calculated using Equation (11) [41].

$$G_i^* = \frac{\sum_{j=1}^n w_{ij}(d) x_j}{\sum_{j=1}^n x_j} \quad (11)$$

where $\{w_{ij}\}$ is an n -by- n symmetrical matrix of 0 or 1 and represents the spatial relations of neighborhood i and the rest neighborhoods; a value of 1 indicates that neighborhood j is a neighbor to neighborhood i while 0 means that j does not neighbor i , which is determined by the distance d between them. x_i and x_j refer to the value of neighborhood i and j , respectively.

This method proportionally compares the sum of a neighborhood and its neighbors to the sum of all neighborhoods and tests if the local sum is significantly different from the expected value. The local G_i^* statistic can directly identify the local hot spots or cold spots of the AAL. Hot spots reflect that the AAL scores of a neighborhood and its neighbors are averagely higher than the expected value while cold spots indicate an opposite situation [17].

3. Results and Discussion

3.1. Exposure of Residential Buildings and Household Properties

The asset value of residential buildings and its spatial distribution in Shanghai can be estimated, based on the area, number of floors and house prices of residential buildings, while the values of household properties and their distribution can be derived, using Equations (1)–(3). The spatial distributions of exposed assets for residential buildings and household properties are mapped by overlay analysis to combine the four extreme flood inundation scenarios with the asset value maps in Shanghai in 2017 (Figure 5).

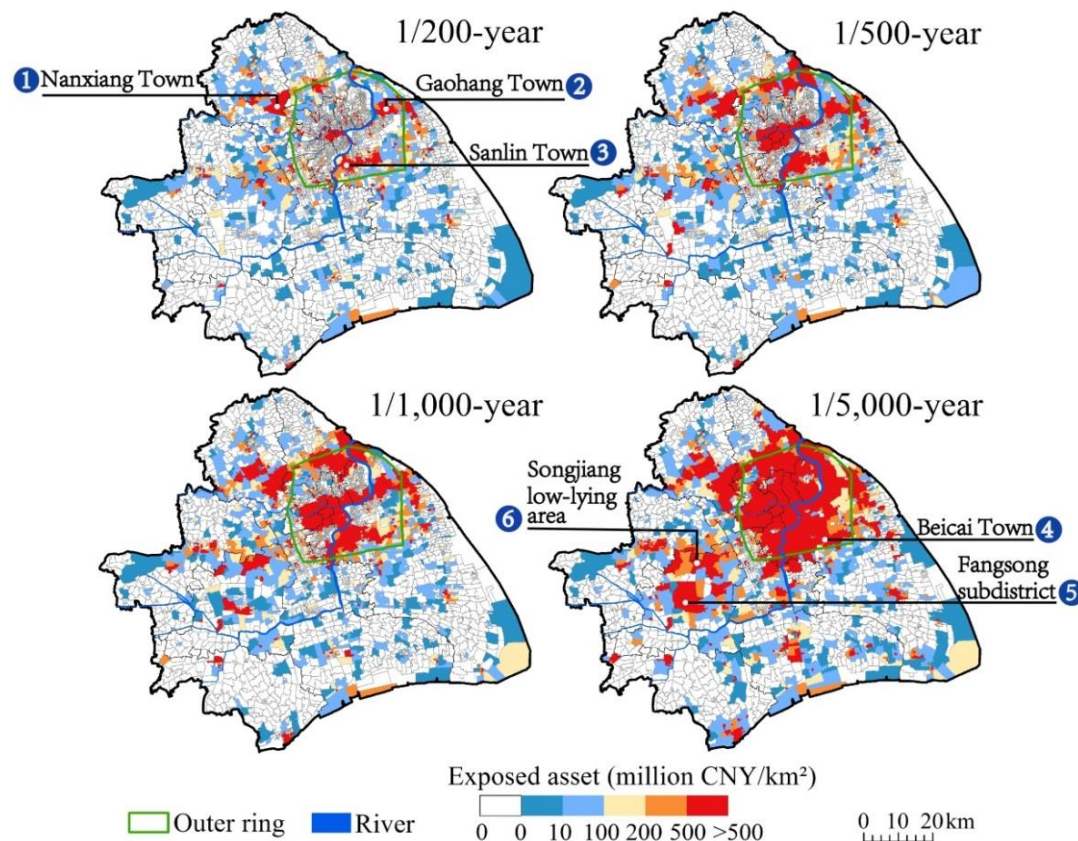


Figure 5. Spatial distributions of exposed total asset value for residential buildings and household properties to extreme flooding under four return periods in the NC level of Shanghai.

Our analysis shows that the exposure increases rapidly as the return periods of storm flooding increases (Table 1). The exposed asset of residential buildings is much larger (accounting for around 95% of the total) than that of household properties (accounting for only about 5%) for all four inundation scenarios. For the 1/5000-year scenario, the exposed assets of residential buildings and household properties are 8.8 times and 8.2 times of those for 1/200-year, respectively, while the area of exposed residential buildings (162.4 km^2) is 6.5 times of that for 1/200-year.

Table 1. Exposure statistics of residential buildings and household properties to extreme flooding under four return periods in Shanghai.

Exposed Asset [Billion CNY]	Return Periods [Years]			
	200	500	1000	5000
Residential buildings	668.6	1893.6	2793.5	5871.8
Household properties	34.9	87.4	131.0	288.6
Total	703.5	1981.0	2924.5	6160.4

Figure 5 shows that the residential buildings and household properties are sporadically exposed to the 1/200-year storm flood, and mainly distributed around both sides of the outer ring (Figure 5). With the increase of the return period, many sporadically exposed areas expand rapidly, and gradually become contiguous. Meanwhile, the exposed extent centered at the Suzhou Creek mouth (① in Figure 1b) has significantly increased in the inner city. For 1/5000-year, two contiguous distribution areas are formed: One is distributed in the main urban area inside and outside the outer ring, another is located at the Songjiang low-lying area (Figure 5) in west Shanghai.

Of 15 districts, Pudong has the largest proportion of exposed assets under four scenarios although it has drops from 43.8% of the total in Shanghai for 1/200-year to greater than 1/4 for 1/5000-year scenario. The exposed residential buildings and household properties caused by a 1/200 storm flood are mainly concentrated in the Pudong and Jiading districts, which account for more than 57% of the total exposed asset. For 1/5000-year, the total exposure in Pudong still accounts for 28.4%, while other districts have more or less exposure distributions with a ratio of less than 9%. In contrast, the total exposed asset in eight downtown districts increases dramatically, which finally accounts for 41.4% for 1/5000-year scenario.

With respect to the subdistrict/township level, the number of subdistricts/towns that have exposed residential buildings and household properties is 173 (82.8%) and 201 (96.2%) for 1/200-year and 1/5000-year events, respectively. For 1/200-year, Nanxiang Town accounts for 8.3% of the total exposure in the Jiading District, Gaohang Towns (7.1%) and Sanlin (7.2%) in Pudong have the largest proportion. For 1/5000-year, Sanlin (3.9%) and Beicai Towns (2.7%) in Pudong, the Fangsong Subdistrict (2.2%) in Songjiang are the most exposed areas (Figure 5).

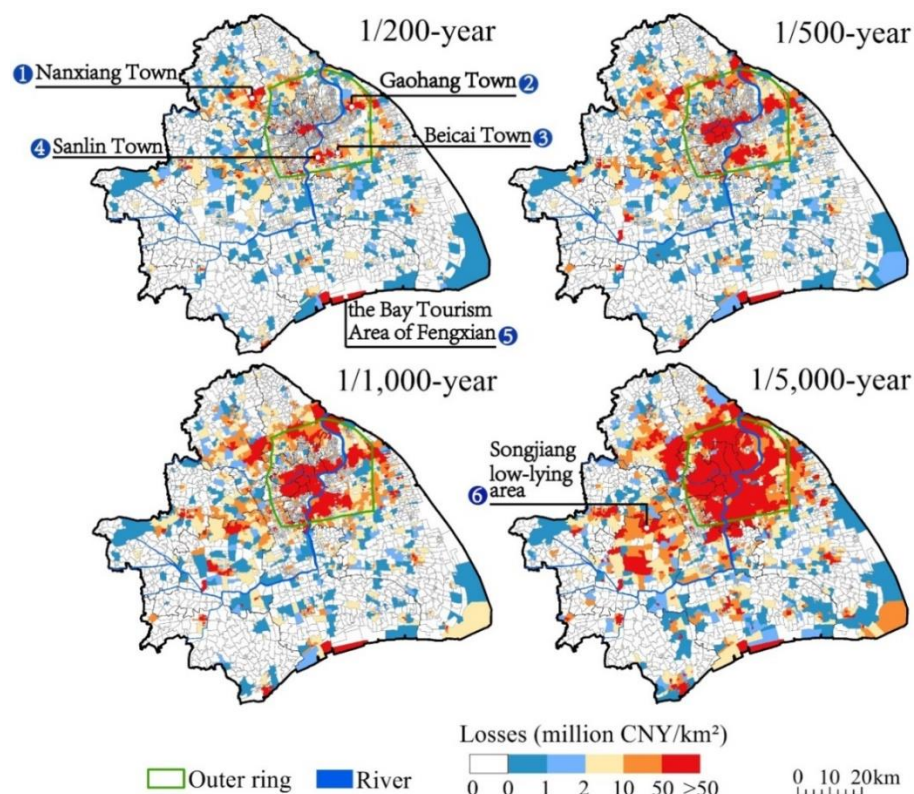
3.2. Losses of Residential Buildings and Household Properties

The direct economic losses and their distribution of residential buildings and household properties caused by extreme flooding under the four return periods can be calculated, using Equations (7)–(9) to combine the exposed assets with the corresponding stage-damage functions (Figure 6).

Figure 6 shows that the spatial patterns of the total losses for residential buildings and household properties are quite similar to exposure (Figure 5) under four storm flood scenarios. The loss, scattered for 1/200-year scenario, rapidly increases in terms of extent and amount with the increase of the return period. For 1/5000-year, the total loss of residential buildings and household properties reaches up to 366 billion CNY (Table 2), is mainly composed by two contiguous areas. One is located in the main urban area and another in the Songjiang low-lying area (Figure 6) in west Shanghai. Under all four scenarios, the losses of residential buildings are approximately 2.7–3.0 times those of household properties (Table 2).

Table 2. Statistics of loss analysis for residential buildings and household properties caused by extreme flooding under four return periods in Shanghai.

Economic Losses [Billion CNY]	Return Periods [Years]			
	200	500	1000	5000
Residential buildings	21.7	71.4	116.0	268.1
Household properties	8.0	24.2	38.6	97.9
Total	29.7	95.6	154.6	366.0

**Figure 6.** Loss distribution of residential buildings and household properties caused by extreme flooding under four return periods in the NC level of Shanghai.

With respect to the loss in each administrative division, of 15 districts, the losses of residential buildings and household properties in Pudong accounts for the largest proportion under four scenarios though it drops from 41.6% for 1/200-year to about 1/4 for the other scenarios. For 1/200-year, the loss is mainly concentrated in the Pudong and Jiading Districts. These two districts account for more than 55.4% of the total loss, while the loss in the inner city is relatively low (21.6%). For 1/5000-year, besides Pudong, losses in Baoshan District is also larger than 10%, while the losses in the inner city significantly increases, with a total loss reaching up to 45.3%. Of 209 subdistricts/towns, the number of those with losses of residential buildings and household properties increases from 173 (82.8%) for 1/200-year to 201 (96.2%) for 1/5000-year scenario. For 1/200-year, five towns (Nanxiang, Gaohang, Beicai, Sanlin and the Bay Tourism Area of Fengxian District in Figure 6) with losses exceeding 5% of the total have an aggregate loss up to 32.8%. For 1/5000-year, the losses in Sanlin (3.8% of the total) and Beicai Towns (2.3%) in Pudong, and Nanxiang Town (2.0%) in Jiading are the largest at the township level (Figure 6).

3.3. Risk and Its Spatial Pattern

3.3.1. Risk Expression

The annual exceedance probability (AEP)-loss curves of extreme flooding for residential buildings, household properties and the summation of the two are plotted respectively (Figure 7a–c), based on the losses under four scenarios. The average annual loss (AAL) is then calculated by Equation (10). The AALs of residential buildings and household properties in Shanghai are 440 million CNY/year (65.4 million USD/year) and 150 million CNY/year (22.3 million USD/year), respectively, with a total of 590 million CNY/year (87.4 million USD/year). Pudong, Baoshan and Huangpu Districts have the highest AAL of 148, 56 and 50 million CNY/year, respectively. The AAL of eight downtown districts in the inner city is up to 290 million CNY/year, accounting for 49% of the total. Figure 8 shows that eight most vulnerable subdistricts/towns scatter throughout the main urban area. Each of them has an AAL larger than 12 million CNY/year, with a total of 124 million CNY/year.

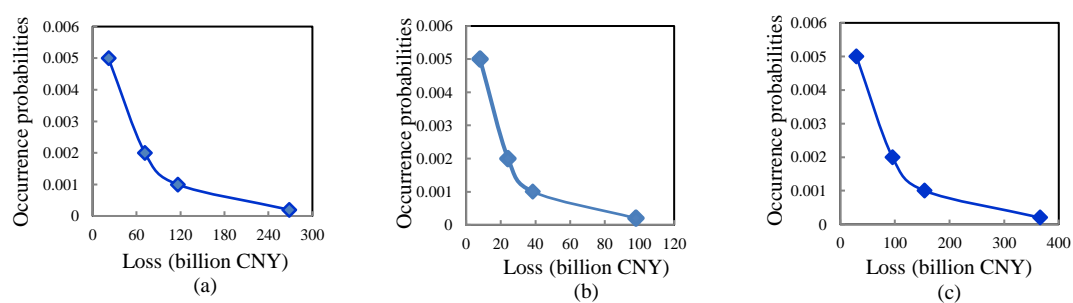


Figure 7. AEP-loss curves of extreme flooding for residential building (a), household properties (b) and the sum of residential buildings and household properties (c) in Shanghai.

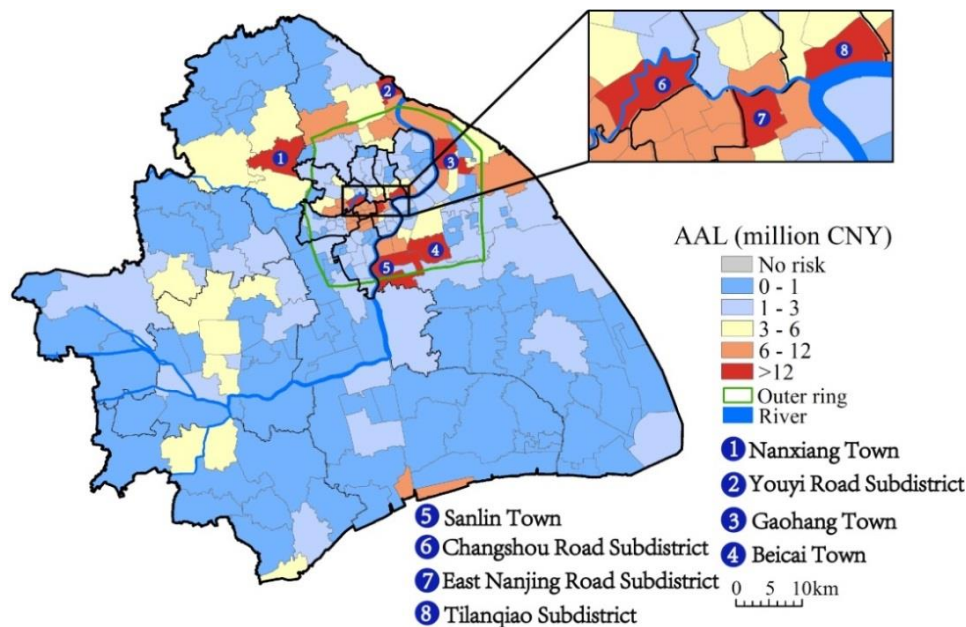


Figure 8. The AAL distribution of residential buildings and household properties at the township level in Shanghai.

3.3.2. Spatial Pattern of the AAL

The result derived from the local Gi* statistic shows a hierarchical pattern for the AAL of residential buildings and household properties in Shanghai (Figure 9). Hot spots and cold spots occupy 1342 (34.6%) and 1238 (31.9%) neighborhoods, respectively. The AAL patterns of hot and cold spots are

similar to the AAL distribution at the township level. A significant hot spot occupies the central city, which was surrounded by cold spots, and then four hotspots centered around Nanxiang, Youyi Road, Gaohang, Beicai subdistricts/towns (①, ②, ③, ④, in Figure 8) situate inside and outside the outer ring (Figure 9). No significant hot spots form in the Songjiang low-lying area in west Shanghai. In contrast, an obvious hot spot is situated around the Bay Tourism Area of Fengxian District along the Hangzhou Bay. These spatial patterns of the AAL reveal the distributions of the higher and lower extreme flood risk in Shanghai.

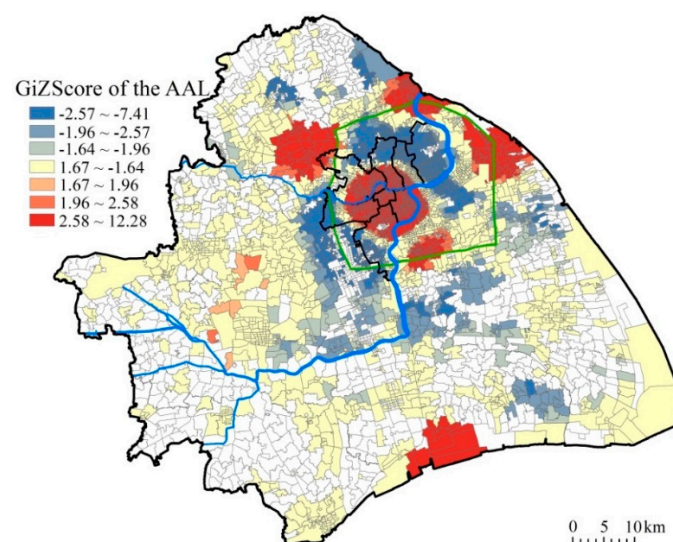


Figure 9. The hot/cold spots of the AAL for resident buildings and household properties at the NC level in Shanghai.

3.4. Discussion

The frequency of fluvial and coastal storm flooding has dropped significantly, while the urban pluvial flooding caused by rainstorms have risen sharply in Shanghai in recent decades [53]. The urban pluvial flooding usually occurs from several times a year to once several years, but its impact and losses are relatively smaller, with direct economic losses ranged from tens of millions CNY to several hundred million CNY [54]. However, extreme flooding, caused synchronously by a typhoon induced storm surge, a high astronomic tide, heavy rain, and a fluvial flood, is categorized as catastrophic disaster with a low probability and high impact, with return periods of a hundred years or even millennium years, and the direct economic loss is usually more than 10 billion CNY [54]. It's the primary risk of flooding to the Shanghai city.

In this work, the inundation maps, exposure of residential buildings and household properties, stage-damage functions all contain a certain degree of uncertainty which propagates through the calculation and accumulates in AEP-loss curves and AAL calculations [55,56]. These sources of uncertainties should be further addressed in future flood risk studies. In addition, Mosimann et al. [30] presented two models, deduced from loss claims on residential buildings, which allow to predict the degree of loss or the monetary loss for household contents based only on corresponding losses on the building structure. The work presented by Mosimann et al. [30] provides a new approach for estimating the vulnerability, losses and risks for household properties caused by flooding in Shanghai. As a preliminary comparison, first, Wu et al. [34] roughly estimated the exposed building asset value of 1868.3 billion CNY, and a total damage of approximately 197.6 billion CNY for a 1/1000-year flood scenario by Ke [1]. Correspondingly, we also used the same scenario to estimate the loss of residential buildings, and the result showed the loss was 176.3 billion CNY. Our result is much larger due mainly to the housing price we used. The average housing price in 2017 used in this work is 54.2 thousand CNY per square meter while the construction cost per square meter of 4197.0 CNY in 2014 was used

in Wu et al. [34]. Second, on 6 August 2005, heavy rain brought by typhoon “Masha” flooded more than 50,000 households, and the direct economic loss was estimated at 1.36 billion CNY [20], which was comparable with our results after extrapolation of the number of inundated households. Third, our results show the loss of household properties accounts for about 27% of the total losses, which is comparable to those found by Mosimann et al. [30] (from 21% to 32%), Thieken et al. [31] (28%) or FOWG [27] (36.5%). In addition, the exposure of household properties is an order of magnitude (around 5% of the total) smaller than that of residential buildings (around 95%), which indicates that household properties are more vulnerable to flooding in general [30]. Despite the uncertainties, this study has presented the flood risk and its spatial pattern for residential buildings and household properties in Shanghai for the first time, which can provide meaningful information for risk-sensitive urban planning and flood risk management in Shanghai [57].

The spatial heterogeneity of extreme flood risk in Shanghai (Figure 9) was mainly caused by spatial distributions of flood severity and the assets of residential buildings and household properties. In the main urban area inside and outside the outer ring, densely distributed the assets together with severe flooding (especially in 1/1000-year and 1/5000-year events) lead to high exposure, losses and risks, with five out of six remarkable hot spots of the AAL distributed there. The northern bank of the Hangzhou Bay and Songjiang depression area are prone to extreme flooding. However, these two regions have relatively lower extreme flood risk due mainly to less urbanization.

A significant hot spot of extreme flood risk is situated in the central city where the most serious land subsidence has occurred since the 20th century [1,4,8,10,58]. It may be severely flooded as the return period of storm flooding increases. In the context of sea level rise and land subsidence, the return period of extreme flooding will greatly decrease [1,2,4,59], the extreme flood risk in the central city may rise rapidly. It is urgently needed to assess the feasibility and cost-benefit of the barrier project near Wusongkou, the mouth of the Huangpu River, and to strengthen the flood control capacity in order to enhance the safety of the inner city. The north bank of the Hangzhou Bay is subject to extreme flooding, it is necessary to implement risk sensitive urban planning, update standards and codes for settlements and infrastructure in the region. Meanwhile, nature-based or hybrid measures should be taken to enhance flood protection along the Hangzhou Bay. Moreover, the Songjiang depression area in the upper reaches of the Huangpu River is also a flood-prone area. When an extreme flooding event occurs, it will be severely flooded there since the upstream flood is difficult to discharge due to the high water level caused by storm surge if it coincides with a high astronomical tide. In addition, the measures to elevate the buildings or adopt waterproof design are also recommended in hot spot areas.

High risk areas of districts and towns, especially the Pudong District, home to the Shanghai free trade zone and a host of world-class business parks in addition to the rapid growth of residential settlements, are crucial to manage the risk of extreme flooding and enhance the flood resilience. In recent decades, the upgrading of flood control projects in Shanghai was all carried out after the occurrence of huge losses caused by extreme floods. Individual extreme flood events (typhoons in 1962, 1974, 1981 and 1997) seem to have had a greater impact on flood protection decision-making in Shanghai [5,44]. However, our study suggests that Shanghai needs to be more proactive in terms of flood protection similar to the Thames Estuary 2100 [60] and New York’s resilience building plan [61] to manage the catastrophic risk and make the city more resilient to extreme flooding.

4. Conclusions

We developed a multidisciplinary approach to analyze the exposure, loss and risk patterns of residential buildings and household properties in Shanghai under extreme flooding scenarios for the first time. The main conclusions are as follows:

- (1) The spatial patterns of exposure and losses for residential buildings and household properties are similar, and characterized as a rapid increase in the extent and amount of exposure and losses with return periods. For 1/5000-year, two contiguous inundation areas are formed, namely, the main urban area and the Songjiang low-lying area in west Shanghai. The exposure of household

properties is an order of magnitude smaller than that of residential buildings, but the loss of household properties accounts for about 27% of the total losses, indicating that household properties are much more vulnerable to flooding.

- (2) The inundated residential building area caused by 1/200-year and 1/5000-year events increases from 24.9 km² to 162.4 km², and the total loss of residential buildings and household properties escalate from 29.7 billion CNY (4.4 billion USD) to 366.0 billion CNY (54.4 billion USD), with widespread impact throughout Shanghai city.
- (3) The AAL of residential buildings and household properties in Shanghai is 590 million CNY/year (87.4 million USD/year), and several hot spots of extreme flood risk are distributed around the main urban area and on the northern bank of the Hangzhou Bay. Pudong is most vulnerable to extreme flooding, where the exposure and AAL for the residential buildings and household properties covers more than 25% of the total in Shanghai. The inner city is also highly threatened by extreme flooding, with an AAL accounting for 49% of the total; in particular, the central city is a most important hot spot of extreme flood risk. Subdistricts/towns and neighborhood committees with the maximum risks are mainly concentrated in the Pudong, Jiading, Baoshan Districts and the inner city. The above administrative divisions and areas are especially required to strengthen flood resilience.

Our results have important implications for risk-sensitive urban planning and development, and risk management in Shanghai. However, we only conducted risk analysis of residential buildings and household properties for extreme flooding. It is urgently needed to analyze the comprehensive risk caused by the extreme flooding in Shanghai in the context of the climate change, sea level rise and subsidence in order to develop strategies for risk-based development and resilience building in Shanghai.

Author Contributions: X.S. analyzed the data and wrote the paper; J.W. conceived and designed the research and edited the paper; M.Z., L.W. and S.D. simulated the extreme storm flood scenarios; Q.K., W.L., Y.S., S.D., B.L., X.L., and H.X. reviewed and edited the paper, K.C. mapped the housing price.

Funding: This research was funded by the National Natural Science Foundation of China (Grant number: 51761135024, 71603168, 41701001, 41871200, and 41601566), National Key Research and Development Plan (Grant number: YS2017YFC1503001), The Netherlands Organization for Scientific Research NWO (Grant number: ALWSD.2016.007), the Science and Technology Commission of Shanghai Municipality (Grant number: 16070502800) and Jiangsu Planned Projects for Postdoctoral Research Funds.

Conflicts of Interest: The authors declare no conflict of interest.

References

1. Ke, Q. Flood Risk Analysis for Metropolitan Areas: A Case Study for Shanghai. Ph.D. Thesis, Delft University of Technology, Delft, The Netherlands, 2014.
2. Wang, J.; Yi, S.; Li, M.Y.; Wang, L.; Song, C.C. Effects of sea level rise, land subsidence, bathymetric change and typhoon tracks on storm flooding in the coastal areas of Shanghai. *Sci. Total Environ.* **2018**, *621*, 228–234. [[CrossRef](#)] [[PubMed](#)]
3. Swiss Reinsurance Company Ltd. *Mind the Risk: A Global Ranking of Cities under Threat from Natural Disasters*; Swiss Reinsurance Company Ltd.: Zurich, Switzerland, 2013; pp. 1–38.
4. Wang, J.; Gao, W.; Xu, S.Y.; Yu, L.Z. Evaluation of the combined risk of sea level rise, land subsidence, and storm surges on the coastal areas of Shanghai, China. *Clim. Chang.* **2012**, *115*, 537–558. [[CrossRef](#)]
5. Xian, S.Y.; Yin, J.; Lin, N.; Oppenheimer, M. Influence of risk factors and past events on flood resilience in coastal megacities: Comparative analysis of NYC and Shanghai. *Sci. Total Environ.* **2018**, *610–611*, 1251–1261. [[CrossRef](#)]
6. Xu, S.Y.; Wang, J.; Shi, C.; Yan, J.P. Research of the natural disaster risk on coastal cities. *Acta Geogr. Sin.* **2006**, *61*, 127–138. (In Chinese) [[CrossRef](#)]
7. Yin, J.; Yu, D.P.; Wilby, R. Modelling the impact of land subsidence on urban pluvial flooding: A case study of downtown Shanghai, China. *Sci. Total Environ.* **2016**, *544*, 744–753. [[CrossRef](#)] [[PubMed](#)]

8. Yin, J.; Yu, D.P.; Yin, Z.E.; Wang, J.; Xu, S.Y. Multiple scenario analyses of Huangpu River flooding using a 1D/2D coupled flood inundation model. *Nat. Hazards* **2013**, *66*, 577–589. [[CrossRef](#)]
9. Cheng, H.Q.; Chen, J.Y.; Chen, Z.J.; Ruan, R.L.; Xu, G.Q.; Zeng, G.; Zhu, J.R.; Dai, Z.J.; Chen, X.Y.; Gu, S.H. Mapping sea level rise behavior in an Estuarine Delta System: A case study along the Shanghai coast. *Engineering* **2018**, *4*, 156–163. [[CrossRef](#)]
10. Yin, J.; Yu, D.P.; Yin, Z.E.; Wang, J.; Xu, S.Y. Modelling the combined impacts of sea-level rise and land subsidence on storm tides induced flooding of the Huangpu River in Shanghai, China. *Clim. Chang.* **2013**, *119*, 919–932. [[CrossRef](#)]
11. Hallegatte, S.; Green, C.; Nicholls, R.J.; Corfee-Morlot, J. Future flood losses in major coastal cities. *Nat. Clim. Chang.* **2013**, *3*, 802. [[CrossRef](#)]
12. Wang, J.; Xu, S.Y.; Ye, M.W.; Huang, J. The MIKE model application to overtopping risk assessment of seawalls and levees in Shanghai. *Int. J. Disaster Risk Sci.* **2011**, *2*, 32–42. [[CrossRef](#)]
13. Nicholls, R.J.; Reeder, T.; Brown, S.; Haigh, I.D. The risks of sea-level rise for coastal cities. In *Climate Change: A Risk Assessment*; King, D., Schrag, D., Zhou, D.D., Qi, Y., Ghosh, A., Eds.; Center for Science and Policy: Cambridge, UK, 2015; pp. 94–98.
14. Shi, Y. The vulnerability assessment of residences in rainstorm waterlogging in cities: A case study of shanghai. *J. Catastrophol.* **2015**, *30*, 94–98. (In Chinese)
15. Yin, J.; Yu, D.P.; Yin, Z.E.; Wang, J.; Xu, S.Y. Modelling the anthropogenic impacts on fluvial flood risks in a coastal mega-city: A scenario-based case study in Shanghai, China. *Landsc. Urban Plan.* **2015**, *136*, 144–155. [[CrossRef](#)]
16. Wang, C.X.; Du, S.Q.; Wen, J.H.; Zhang, M.; Gu, H.H.; Shi, Y.; Xu, H. Analyzing explanatory factors of urban pluvial floods in Shanghai using geographically weighted regression. *Stoch. Env. Res. Risk A* **2017**, *31*, 1777–1790. [[CrossRef](#)]
17. Gu, H.H.; Du, S.Q.; Liao, B.G.; Wen, J.H.; Wang, C.X.; Chen, R.S.; Bo, C. A hierarchical pattern of urban social vulnerability in Shanghai, China and its implications for risk management. *Sustain. Cities Soc.* **2018**, *41*, 170–179. [[CrossRef](#)]
18. Quan, R.S. Research on Risk Assessment of Rainstorm Waterlogging Disaster in Typical City. Ph.D. Thesis, East China Normal University, Shanghai, China, 2012. (In Chinese).
19. Wen, J.H.; Huang, H.; Chen, K.; Ye, X.L.; Hu, H.Z.; Hua, Z.Y. Probabilistic community-based typhoon disaster risk assessment: A case of Fululi community, Shanghai. *Sci. Geogr. Sin.* **2012**, *32*, 348–355. (In Chinese) [[CrossRef](#)]
20. Yin, Z.E.; Yin, J.; Xu, S.Y.; Wen, J.H. Community-based scenario modelling and disaster risk assessment of urban rainstorm waterlogging. *J. Geogr. Sci.* **2011**, *21*, 274–284. [[CrossRef](#)]
21. Aerts, J.C.J.H.; Lin, N.; Wouter Botzen, W.J.; Emanuel, K.; De Moel, H. Low-probability flood risk modeling for New York City. *Risk Anal.* **2013**, *33*, 772–788. [[CrossRef](#)]
22. Huang, X.L.; Li, X.D.; Wen, J.H.; Li, W.J.; Du, S.Q. Measuring the economic losses and ripple effects of Shanghai automobile firms under extreme flood scenarios. *Geogr. Res.* **2017**, *36*, 1801–1816. (In Chinese) [[CrossRef](#)]
23. Li, W.J.; Wen, J.H.; Xu, B.; Li, X.D.; Du, S.Q. Integrated assessment of economic losses in manufacturing industry in Shanghai metropolitan area under an extreme storm flood scenario. *Sustainability* **2018**, *11*, 126. [[CrossRef](#)]
24. Liu, K.C. An estimation for the probable maximum typhoon surges in Shanghai Harbour. *Coast. Eng.* **1984**, *3*, 19–29. (In Chinese)
25. Zhu, Y.S. Analysis and Management of Flood Risk (Tide) Safety Risk in Shanghai. Available online: http://jhe.ches.org.cn/jhe/ch/reader/view_html.aspx?file_no=2002080021 (accessed on 6 June 2019). (In Chinese).
26. Bermúdez, M.; Zischg, A.P. Sensitivity of flood loss estimates to building representation and flow depth attribution methods in micro-scale flood modelling. *Nat. Hazards* **2018**, *92*, 1633–1648. [[CrossRef](#)]
27. Federal Office for Water and Geology (FOWG). *Bericht über die Hochwasserereignisse 2005*; Federal Office for Water and Geology: Bern, Switzerland, 2005.
28. Federal Office for the Environment (FOEN). *EconoMe 4.0. Wirksamkeit und Wirtschaftlichkeit von Schutzmassnahmen gegen Naturgefahren*; Federal Office of Environment FOEN: Bern, Switzerland, 2015.
29. Kreibich, H.; Seifert, I.; Merz, B.; Thieken, A.H. Development of FLEMOcs—A new model for the estimation of flood losses in the commercial sector. *Hydrol. Sci. J.* **2010**, *55*, 1302–1314. [[CrossRef](#)]

30. Mosimann, M.; Frossard, L.; Keiler, M.; Weingartner, R.; Zischg, P.A. A robust and transferable model for the prediction of flood losses on household contents. *Water* **2018**, *10*, 1596. [CrossRef]
31. Thieken, A.H.; Müller, M.; Kreibich, H.; Merz, B. Flood damage and influencing factors: New insights from the August 2002 flood in Germany. *Water Resour. Res.* **2005**, *41*. [CrossRef]
32. Shanghai Municipal Statistics Bureau. Shanghai Statistical Yearbook 2017. Available online: <http://www.stats-sh.gov.cn/html/sjfb/201801/1001529.html> (accessed on 23 April 2019). (In Chinese)
33. Shi, Y. Research on Vulnerability Assessment of Cities on The Disaster Scenario: A Case of Shanghai City. Ph.D. Thesis, East China Normal University, Shanghai, China, 2010. (In Chinese).
34. Wu, J.D.; Ye, M.Q.; Xu, W.; Koks, E. Building asset value mapping in support of flood risk assessments: A case study of Shanghai, China. *Sustainability* **2019**, *11*, 971. [CrossRef]
35. Wang, L.Y.; Zhang, M.; Wen, J.H.; Chong, Z.T.; Ye, Q.H.; Ke, Q. Simulation of extreme compound coastal flooding in Shanghai. *Adv. Water Sci.* **2019**, in press (In Chinese)
36. Global Facility for Disaster Reduction and Recovery (GFDRR). *Open Data for Resilience Initiative: Planning an Open Cities Mapping Project*; World Bank: Washington, DC, USA, 2015.
37. Chapi, K.; Singh, V.P.; Shirzadi, A.; Shahabi, H.; Bui, D.T.; Pham, B.T.; Khosravi, K. A novel hybrid artificial intelligence approach for flood susceptibility assessment. *Environ. Model. Softw.* **2017**, *95*, 229–245. [CrossRef]
38. Global Facility for Disaster Reduction and Recovery (GFDRR). *Machine Learning for Disaster Risk Management*; The World Bank: Washington, DC, USA, 2018.
39. Tehrany, M.S.; Pradhan, B.; Mansor, S.; Ahmad, N. Flood susceptibility assessment using GIS-based support vector machine model with different kernel types. *Catena* **2015**, *125*, 91–101. [CrossRef]
40. Chen, K.; Shan, X.M.; Huang, Y.Q.; Du, S.Q.; Wen, J.H. Housing price mapping through machine learning and online data-A case study in Shanghai. *Int. J. Geo-Inf.* **2019**, submitted for publication.
41. Getis, A.; Ord, K. The analysis of spatial association by use of distance statistics. *Geogr. Anal.* **1992**, *24*, 189–206. [CrossRef]
42. Chen, Z.L.; Wang, J.; Liu, M.; Yu, L.Z.; Xu, S.Y. Characteristics of main natural disasters and coping strategies in Shanghai. *J. East China Norm. Univ. Nat. Sci.* **2008**, *5*, 116–125. (In Chinese) [CrossRef]
43. China National Commission for Disaster Reduction. *The Standards of Model Community of Integrated Disaster Governance*; Office of China National Commission for Disaster Reduction: Beijing, China, 2010.
44. Gu, X.X. Review and prospect of flood wall construction on Huangpu river in Shanghai in the past 50 years (part I). *Shanghai Water* **2005**, *21*, 15–18. (In Chinese)
45. Yin, J. Study on the Risk Assessment of Typhoon Storm Tide in China Coastal Area. Ph.D. Thesis, East China Normal University, Shanghai, China, 2011. (In Chinese).
46. Zhang, M.; Townend, I.; Cai, H.; He, J.; Mei, X. The influence of seasonal climate on the morphology of the mouth-bar in the Yangtze Estuary, China. *Cont. Shelf Res.* **2018**, *153*, 30–49. [CrossRef]
47. Zhang, M.; Townend, I.H.; Cai, H.; Zhou, Y. Seasonal variation of tidal prism and energy in the Changjiang River Estuary: A numerical study. *Chin. J. Oceanol. Limnol.* **2016**, *34*, 219–230. [CrossRef]
48. Ke, Q.; Jonkman, S.N.; van Gelder, P.H.A.J.M.; Bricker, J.D. Frequency analysis of storm-surge-induced flooding for the Huangpu River in Shanghai, China. *J. Mar. Sci. Eng.* **2018**, *6*, 70. [CrossRef]
49. Chen, T.Q.; Guestrin, C. XGBoost: A scalable tree boosting system. In Proceedings of the 22nd ACM SIGKDD International Conference on Knowledge Discovery and Data Mining, San Francisco, CA, USA, 13–17 August 2016; pp. 785–794.
50. Kunreuther, H.; Useem, M. *Learning from Catastrophes: Strategies for Reaction and Response*; Wharton School Publishing: New York, NY, USA, 2009.
51. Lamond, J.; Proverbs, D.; Hammond, F. The impact of flooding on the price of residential property: A transactional analysis of the UK Market. *Hous. Stud.* **2010**, *25*, 335–356. [CrossRef]
52. Zhang, Z.G. Research on Rainstorm Waterlogging Risk Assessment of Urban Communities-A Case of Jinsha Community. Ph.D. Thesis, Shanghai Normal University, Shanghai, China, 2014.
53. Du, S.Q.; Gu, H.H.; Wen, J.H.; Chen, K.; Rompaey, A.V. Detecting flood variations in Shanghai over 1949–2009 with Mann-Kendall tests and a newspaper-based database. *Water* **2015**, *7*, 1808–1824. [CrossRef]
54. Wen, J.H.; Du, S.Q.; Xu, H.; Yan, J.P.; Yao, D.J.; Wang, C.X. Research on flood hazard and risk management in Shanghai. In Proceedings of the 2016 National Forum on Integrated Disaster Risk Management and Sustainable Development Forum, Beijing, China, 10 May 2016; pp. 118–129. (In Chinese).

55. Moel, H.D.; Aerts, J.C.J.H. Effect of uncertainty in land use, damage models and inundation depth on flood damage estimates. *Nat. Hazards* **2011**, *58*, 407–425. [[CrossRef](#)]
56. Moel, H.D.; Bouwer, L.M.; Aerts, J.C.J.H. Uncertainty and sensitivity of flood risk calculations for a dike ring in the south of the Netherlands. *Sci. Total Environ.* **2014**, *473–474*, 224–234. [[CrossRef](#)]
57. UNISDR. *How to Make Cities More Resilient: A Handbook for Local Government Leaders*; United Nations: Geneva, Switzerland, 2017; pp. 30–80.
58. Syvitski, J.P.M.; Overeem, A.J.K.I.; Hutton, E.W.H.; Hannon, M.T.; Brakenridge, G.R.; Day, J.; Vörösmarty, C.; Saito, Y.; Giosan, L.; Nicholls, R.J. Sinking deltas due to human activities. *Nat. Geosci.* **2009**, *2*, 681–686. [[CrossRef](#)]
59. Church, J.A.; Clark, P.U.; Cazenave, A.; Gregory, J.M.; Jevrejeva, S.; Levermann, A.; Merrifield, M.A.; Milne, G.A.; Nerem, R.S.; Nunn, P.D. Sea level change. In *Climate Change 2013: The Physical Science Basis*; Cambridge University Press: Cambridge, UK; New York, NY, USA, 2013.
60. Ranger, N.; Reeder, T.; Lowe, J. Addressing ‘deep’ uncertainty over long-term climate in major infrastructure projects: Four innovations of the Thames Estuary 2100 Project. *EURO J. Decis. Process.* **2013**, *1*, 233–262. [[CrossRef](#)]
61. The City of New York. *A Stronger, More Resilient New York*; PlaNYC: New York, NY, USA, 2013; pp. 1–2.



© 2019 by the authors. Licensee MDPI, Basel, Switzerland. This article is an open access article distributed under the terms and conditions of the Creative Commons Attribution (CC BY) license (<http://creativecommons.org/licenses/by/4.0/>).